[9] K.M. Prise, M. Folkard, B.D. Michael, Bystander response induced by low LET radiation, Oncogene 22 (2003) 7043–7049.
[10] Y. Kinashi, S. Masunaga, K. Nagata, M. Suzuki, S. Takahashi, K. Ono, A bystander effect observed in boron neutron capture therapy: a study of the induction of mutations in the HPRT locus, Int. J. Radiat. Oncol. Biol. Phys. 68 (2007) 508–514.
[11] G. Kashino, K.M. Prise, K. Suzuki, N. Matsuda, S. Kodama, M. Suzuki, K. Nagata, Y. Kinashi, S. Masunaga, K. Ono, M. Watanabe, Effective suppression of bystander effects by DMSO treatment of irradiated CHO cells, J. Radiat. Res. 48 (2007) 197–204.
[12] I. Yamamoto, S. Suga, Y. Mitoh, M. Tanaka, N. Muto, Antiscorbutic activity of L-ascorbic acid 2-gluciside and its availability as a vitamin C supplement in normal rats and guinea pigs, J. Pharmacobiodyn. 13 (1990) 688–695.
[13] A. Tai, Y. Fujitani, K. Matsumoto, D. Kawasaki, I. Yamamoto, Bioability of a series of novel acylated ascorbic acid derivatives, 6-O-acyl-2-O-α-D-glucopyranosyl-L-ascorbic acids, as an ascorbic acid supplement in rats and guinea pigs, Biosci. Biotechnol. Biochem. 66 (2002) 1628–1634.
[14] L.V. d'Uscio, S. Milstien, D. Richardson, L. Smith, Z.S. Katusic, Long-term Vitamin C treatment increase vascular tetrahydrobiopterin levels and nitric oxide synthase activity, Circulat. Res. 92 (2003) 88–95.
[15] Y. Kinashi, K. Ono, M. Abe, The micronucleus assay of lymphocytes is a useful predictive assay of the radiosensitivity of normal tissue: a study of three inbred strains of mice, Radiat. Res. 148 (1997) 341–347.
[16] H. Waldmann, S. Cobbold, I. Lefkovits, Limiting dilution analysis, in: G.G.B. Klaus (Ed.), Lymphocytes, A Practical Approach, IRL, Oxford, 1987, pp. 163–188.
[17] F. Fenech, A.A. Morley, Cytokinesis-block micronucleus method in human lymphocytes: effect of in vivo aging and low dose X-irradiation, Mutat. Res. 161 (1986) 193–198.
[18] T. Kageji, S. Nagahiro, S. Uyama, Y. Mizobuchi, Y. Nakagawa, Clinical review of BNCT using mixed neutron beam in patients with malignant glioma, in: W. Sauerwein, R. Moss, A. Wittig (Eds.), Research and Development in Neutron Capture Therapy Monduzzi Editore S.p.A., Bologna, Italy, 2002, pp. 1085–1091.
[19] S.A. Lorimore, P.J. Coates, G.E. Scobie, G. Milne, E.G. Wright, Inflammatory-type responses after exposure to ionizing radiation in vivo: a mechanism for radiation-induced bystander effects? Oncogene 20 (2001) 7085–7095.
[20] L.E. Lambert, D.M. Paulnock, Modulation of macrophage function by γ-irradiation; Acquisition of the primed cell intermediate stage of macrophage tumoricidal action pathway, J. Immunol. 139 (1987) 2834–2841.
[21] G. McLennan, L.W. Oberley, A.P. Author, The role of oxygen-derived free radicals in radiation-induced damage and death of nondividing eukaryotic cells, Radiat. Res. 84 (1980) 122–132.
[22] K.H. Kohn, M.M. Kallman, The influence of strain on acute X-ray lethality in the mouse: LD50 and death rate studies, Radiat. Res. 5 (1956) 309–317.
[23] T.H. Roderic, The response of twenty-seven inbred strains of mice to daily doses of whole-body X-irradiation, Radiat. Res. 120 (1963) 631–639.
[24] R. Hardmeier, H. Hoeger, S. Fang-Kircher, A. Khoschsorur, G. Lubic, Transcription and activity of antioxidant enzymes after ionizing irradiation in radiation-resistant and radiation-sensitive mice, Proc. Natl. Acad. Sci. U.S.A. 94 (1997) 7572–7576.
[25] Y. Kinashi, Y. Sakurai, S. Masunaga, M. Suzuki, M. Akaboshi, K. Ono, Dimethyl sulfoxide protects against thermal and epithermal neutron-induced cell death and mutagenesis of Chinese hamster ovary (CHO) cells, Int. J. Radiat. Oncol. Biol. Phys. 47 (2000) 1371–1378.
[26] Y. Kinashi, Y. Sakurai, S. Masunaga, M. Suzuki, K. Nagata, K. Ono, Ascorbic acid reduced mutagenicity at the HPRT locus in CHO cells against thermal neutron radiation, Appl. Radiat. Isotopes 61 (2004) 929–932.
[27] T. Harada, G. Kashino, K. Suzuki, N. Matsuda, S. Kodama, M. Watanabe, Different involvement of radical species in irradiated and bystander cells, Int. J. Radiat. Biol. 84 (2008) 809–814.
[28] E. Gwyneth, S.A. Watson, A. Lorimore, D.A. Macdonald, E.G. Wright, Chromosomal instability in unirradiated cells induced in vivo by a bystander effect of ionizing radiation, Cancer Res. 60 (2000) 5608–5611.
[29] I. Koturbash, A. Boyko, R. Rodriguez-Juarez, R.J. MacDonald, V.P. Tryndyak, I. Kovalchuk, I.P. Pogribny, O. Kovalchuk, Role of epigenetic effects in maintenance of long-term persistent bystander effect in spleen in vivo, Carcinogenesis 28 (2007) 1831–1838.

Jpn J Radiol (2010) 28:132–142
DOI 10.1007/s11604-009-0397-1

ORIGINAL ARTICLE

Influence of manipulating hypoxia in solid tumors on the radiation dose-rate effect in vivo, with reference to that in the quiescent cell population

**Shin-ichiro Masunaga · Ryoichi Hirayama
Akiko Uzawa · Genro Kashino · Takushi Takata
Hiroki Tanaka · Minoru Suzuki · Yuko Kinashi
Yong Liu · Sachiko Koike · Koichi Ando · Koji Ono**

Received: May 19, 2009 / Accepted: November 9, 2009

Abstract
Purpose. The aim of this study was to clarify the effect of manipulating intratumor hypoxia on radiosensitivity under reduced dose-rate (RDR) irradiation.
Materials and methods. Tumor-bearing mice were continuously given 5-bromo-2′-deoxyuridine (BrdU) to label all proliferating (P) cells. They received γ-rays or accelerated carbon-ion beams at high dose-rate (HDR) or RDR with or without tumor clamping to induce hypoxia. Some mice without clamping received nicotinamide, an acute hypoxia-releasing agent or misonidazole, a hypoxic cell radio-sensitizer before irradiation. The responses of quiescent (Q) and total (= P + Q) cells were assessed by the micronucleus frequency using immunofluorescence staining for BrdU.
Results. The clearer decrease in radiosensitivity in Q than total cells after RDR γ-ray irradiation was suppressed with carbon-ion beams, especially with a higher linear energy transfer value. Repressing the decrease in the radiosensitivity under RDR irradiation through keeping tumors hypoxic during irradiation and enhancing the decrease in the radiosensitivity by nicotinamide were clearer with γ-rays and in total cells than with carbon-ion beams and in Q cells, respectively. Inhibiting the decrease in the radiosensitivity by misonidazole was clearer with γ-rays and in Q cells than with carbon-ion beams and in total cells, respectively.
Conclusion. Manipulating hypoxia during RDR as well as HDR irradiation influences tumor radiosensitivity, especially with γ-rays.

Key words Dose-rate effect · Manipulating hypoxia · Quiescent cell · Carbon-ion beams · γ-Rays

S. Masunaga (✉) · G. Kashino · M. Suzuki · Y. Liu · K. Ono
Particle Radiation Oncology Research Center, Research Reactor Institute, Kyoto University, 2-1010 Asashiro-nishi, Kumatori-cho, Sennan-gun, Osaka 590-0494, Japan
Tel. +81-72-451-2406, 2487; Fax +81-72-451-2627
e-mail: smasuna@rri.kyoto-u.ac.jp

R. Hirayama · A. Uzawa · S. Koike
Heavy-Ion Radiobiology Research Group, Research Center for Charged Particle Therapy, National Institute of Radiological Sciences, Chiba, Japan

T. Takata
Wakasawan Energy Research Center, Tsuruga, Fukui, Japan

H. Tanaka
Radiation Medical Physics, Research Reactor Institute, Kyoto University, Kumatori, Osaka, Japan

Y. Kinashi
Radiation Safety and Control, Research Reactor Institute, Kyoto University, Kumatori, Osaka, Japan

K. Ando
Heavy Ion Medical Center, Gunma University, Maebashi, Japan

Introduction

Intensity modulated radiotherapy (IMRT) and stereotactic irradiation have come into common usage as radiotherapy techniques for treating malignancies. Both modalities generally use multiple arc or fixed-portal radiation beams, and radiation beams are exposed intermittently. These techniques often require 30 min or longer in one treatment session for precise positioning

of patients.[1,2] Prolongation of irradiation time may reduce a radiation effect and evokes a major concern for the dose rate effect. Thus, it is needed to clarify the effect of the reduction of dose rate on the radiosensitivity of tumors in vivo.

When using low linear energy transfer (LET) radiation, lowering the dose rate is thought to reduce late effects in normal tissue much more than it decreases tumor control. Thus, the "therapeutic ratio" increases as the dose rate decreases because the therapeutic ratio is equal to the ratio of tumor control to normal tissue complications. Furthermore, the difference between early and late effects for low dose-rate radiotherapy, as well as improving the therapeutic ratio, allows complete treatment in a short period of time, minimizing the effects of tumor repopulation. In other words, decreasing the dose rate increases the therapeutic ratio, limited only by tumor cell repopulation.[3] This is the primary rationale for low dose-rate radiotherapy using low-LET radiation. High-LET radiation is more effective than low-LET X- or γ-radiation at inducing biological damage. High-LET radiation results in a greater relative biological effectiveness (RBE) value for cell killing, a reduced oxygen effect, and a reduced dependence on the cell cycle and the irradiation dose rate.[4]

Manipulating hypoxia in solid tumors during irradiation apparently influences tumor radiosensitivity under high-dose-rate (HDR) irradiation using low-LET radiation.[5] However, its significance in solid tumors irradiated at a reduced dose rate (RDR) is less clear in vivo, whether low- or high-LET radiation is employed.

Many cells in solid tumors are quiescent in situ but still clonogenic.[6] The quiescent (Q) tumor cells are more resistant to low-LET radiation because of their larger hypoxic fraction and greater capacity to recover from potentially lethal damage (PLD) than proliferating (P) tumor cells. The rationale for low-dose-rate radiotherapy does not take into account the response of Q tumor cells at all.

Thus, in this study, we tried to elucidate the effect of manipulating hypoxia in irradiated solid tumors at an RDR with low-LET γ-rays or high-LET 290 MeV/u accelerated carbon-ion beams in vivo, compared with HDR irradiation. Furthermore, the responses of the total (= P + Q) and Q cell populations in irradiated solid tumors were separately detected with the method for selectively detecting the response of Q cells in solid tumors.[7] This is the first attempt to clarify the direct relation between the irradiation dose rate effect and the oxygen effect in vivo, referring to the response of the Q cell population in irradiated solid tumors.

Materials and methods

Mice and tumors

Squamous cell carcinoma cell line VII (SCC VII) derived from C3H/He mice was maintained in vitro in Eagle's minimum essential medium supplemented with 12.5% fetal bovine serum. The tumor cells (1.0×10^5) were inoculated subcutaneously into the left hind leg of 9-week-old syngeneic female C3H/He mice (Japan Animal Co., Osaka, Japan). Fourteen days later, the tumors, approximately 1 cm in diameter, were employed for experimental treatment, and the body weight of the tumor-bearing mice was 22.1 ± 2.3 g (mean ± SD). Mice were handled according to the Recommendations for Handling of Laboratory Animals for Biomedical Research, compiled by the Committee on Safety Handling Regulations for Laboratory Animal Experiments. Incidentally, the p53 of SCC VII tumor cells is the wild type.[7]

Labeling with 5-bromo-2′-deoxyuridine

Nine days after the inoculation, miniosmotic pumps (Durect, Cupertino, CA, USA) containing 5-bromo-2′-deoxyuridine (BrdU) dissolved in physiological saline (250 mg/ml) were implanted subcutaneously to label all P cells for 5 days. The percentage of labeled cells after continuous labeling with BrdU was 55.3% ± 4.5% and reached a plateau at this stage. Therefore, tumor cells not incorporating BrdU after continuous labeling were regarded as Q cells.

Treatment

After the labeling with BrdU, tumor-bearing mice underwent γ-ray or accelerated carbon-ion whole-body irradiation, with the animal held in a specially designed device made of acrylic resin with the tail or all four legs firmly fixed with adhesive tape with no anesthetic. Some tumors were made totally hypoxic by clamping the proximal end 15 min before irradiation.[7] This clamping for 15 min did not influence clonogenic cell survival or the level of micronucleation. γ-Rays were delivered with a cobalt-60 γ-ray irradiator at a dose rate of 2.5 or 0.039 Gy/min.

Carbon-12 ions were accelerated up to 290 MeV/u by the synchrotron of the Heavy Ion Medical Accelerator installed at National Institute of Radiological Sciences in Chiba, Japan. The dose rate was regulated through a beam attenuation system, and irradiation was conducted using horizontal carbon beams with a dose rate of 1.0 or 0.035 Gy/min. The LET of the carbon ion beam with the

6-cm spread-out Bragg peak (SOBP) ranges from 14 keV/μm to >200 keV/μm, depending on depth. A desired LET beam was obtained by selecting the depth along the beam path using a Lucite range shifter. LETs of 18 and 50 keV/μm at the middle of the plateau and the SOBP, respectively, were employed here.[8]

Irradiated tumor-bearing mice were divided into four groups: group I, tumors were excised immediately after irradiation only under aerated conditions; group II, tumors were kept totally hypoxic during irradiation, then excised immediately after irradiation; group III, tumor-bearing mice received intraperitoneal administration of an acute hypoxia-releasing agent, nicotinamide (1000 mg/kg mouse weight) dissolved in physiological saline 60 min before irradiation, after which the tumors were excised immediately under aerated conditions; group IV, tumor-bearing mice received intraperitoneal administration of a hypoxic cell radiosensitizer, misonidazole (1000 mg/kg of mouse weight) dissolved in physiological saline 30 min before irradiation, after which the tumors were excised immediately under aerated conditions. All the doses employed, sequences, and timing for nicotinamide, misonidazole, and irradiation were appropriate enough to function completely.[9,10] Each treatment group also included mice not pretreated with BrdU.

Immunofluorescence staining of BrdU-labeled cells and micronucleus assay

Tumors excised from the mice given BrdU were minced and trypsinized [0.05% trypsin and 0.02% ethylenediaminetetraacetic acid (EDTA) in phosphate-buffered saline (PBS), 37°C, 20 min]. Tumor cell suspensions were incubated for 72 h in tissue culture dishes containing complete medium and cytochalasin-B of 1.0 μg/ml to inhibit cytokinesis while allowing nuclear division. The cultures were then trypsinized, and cell suspensions were fixed. After centrifugation of fixed cell suspensions, the cell pellet was resuspended with cold Carnoy's fixative (ethanol/acetic acid ratio was 3:1 vol/vol). The suspension was placed on a glass microscope slide, and the sample was dried at room temperature. The slides were treated with 2 M hydrochloric acid for 60 min at room temperature to dissociate the histones and partially denature the DNA. The slides were immersed in borax-borate buffer (pH 8.5) to neutralize the acid. BrdU-labeled tumor cells were detected by indirect immunofluorescence staining using a monoclonal anti-BrdU antibody (Becton Dickinson, San Jose, CA, USA) and a fluorescein isothiocyanate (FITC)-conjugated anti-mouse immunoglobulin G (IgG) antibody (Sigma, St. Louis, MO, USA). To observe the double staining of tumor cells with green-emitting FITC and red-emitting propidium iodide (PI), cells on the slides were treated with PI in PBS (2 μg/ml) and monitored under a fluorescence microscope.

The micronucleus (MN) frequency in cells not labeled with BrdU could be examined by counting the micronuclei in the binuclear cells that showed only red fluorescence. The MN frequency was defined as the ratio of the number of micronuclei in the binuclear cells to the total number of binuclear cells observed.[7] The MN frequency has already been shown to be a tool for detecting radiosensitivity to carbon-ion beams.[11]

The ratios obtained in tumors not pretreated with BrdU indicated the MN frequency at all phases in the total tumor cell population. More than 400 binuclear cells were counted to determine the MN frequency.

Clonogenic cell survival assay

The clonogenic cell survival assay was also performed in the mice given no BrdU using an in vivo–in vitro assay method. Tumors were disaggregated by stirring for 20 min at 37°C in PBS containing 0.05% trypsin and 0.02% EDTA. The cell yield was $4.5 \pm 1.1 \times 10^7$/g tumor weight.

As stated above, the MN frequencies for Q cells were obtained from nonlabeled tumor cells after continuous BrdU labeling. The MN frequencies and surviving fractions (SFs) for the total cell population were obtained from cells in tumors not pretreated with BrdU. Thus, there was no effect of interaction between BrdU and irradiation on the values of MN frequency and SFs. More than three tumor-bearing mice were used to assess each set of conditions, and each experiment was repeated at least twice.

To examine the differences between pairs of values, Student's *t*-test was used when variances of the two groups could be assumed to be equal. Otherwise, the Welch *t*-test was used.

Results

The plating efficiency and MN frequency at 0 Gy are shown in Table 1. The plating efficiency was significantly smaller for the combination with MISO than for any other condition in the total cell population. In both the total and Q cell populations, the MN frequency significantly increased in the following order: absolute control < totally hypoxic conditions < combination with nicotinamide < combination with misonidazole. Furthermore, the MN frequency was significantly higher for the Q cell population than for the total cell population under all conditions.

Table 1. Plating efficiency and micronucleus frequency at 0 Gy

Parameter	Total tumor cells	Quiescent cells
Plating efficiency (%)		
Absolutely controlled	53.7 ± 8.5	—
Totally hypoxic	50.1 ± 7.0	—
+ Nicotinamide	46.8 ± 0.6	—
+ Misonidazole	31.2 ± 7.7	
Micronucleus frequency		
Absolutely controlled	0.043 ± 0.005	0.063 ± 0.009
Totally hypoxic	0.058 ± 0.006	0.073 ± 0.010
+ Nicotinamide	0.073 ± 0.009	0.119 ± 0.014
+ Misonidazole	0.093 ± 0.011	0.152 ± 0.018

Results are the mean ± standard deviation

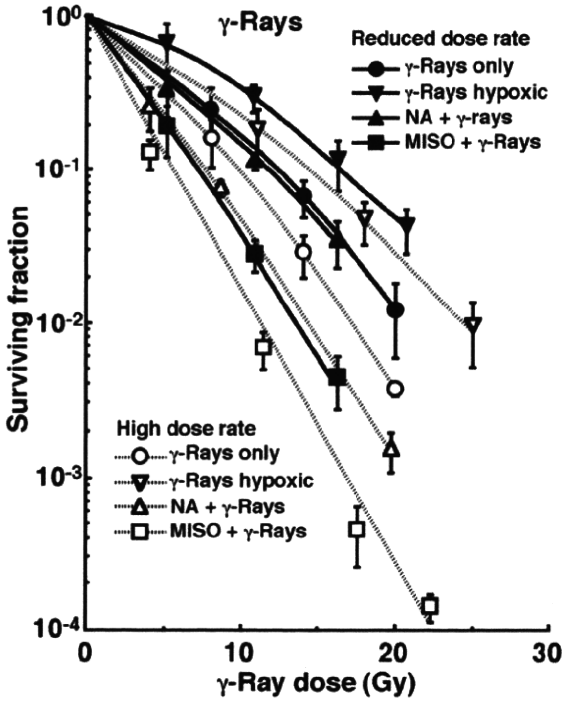

Fig. 1. Cell survival curves for the total tumor cell population as a function of the radiation dose after γ-ray irradiation. *Open* and *solid symbols* represent the surviving fractions after high-dose-rate and reduced-dose-rate γ-ray irradiation, respectively. *Circles*, *reversed triangles*, *triangles*, and *squares* represent the surviving fractions after aerobic irradiation without any drug, irradiation under totally hypoxic conditions, aerobic irradiation after nicotinamide (*NA*) loading, and aerobic irradiation after misonidazole (*MISO*) loading, respectively. *Bars* represent standard errors

Cell survival curves for the total tumor cells as a function of radiation dose after γ-ray irradiation are shown in Fig. 1. For both HDR and RDR irradiation, the SFs decreased in the following order: irradiation under totally hypoxic conditions > aerobic irradiation without any drug > irradiation after nicotinamide loading > irradiation after misonidazole loading. The SFs under all conditions increased as the dose rate of radiation decreased, especially after nicotinamide loading.

Cell survival curves for the total tumor cells as a function of radiation dose after accelerated carbon-ion beam irradiation with an LET of 18 and 50 keV/μm are shown in the left and right panels of Fig. 2, respectively. For both HDR and RDR irradiation, the SFs decreased in the same order as for γ-ray irradiation, but the degree of change was reduced, especially with 50 keV/μm carbon-ion beams. The increases in the SF with the decrease in dose rate were suppressed compared with γ-ray irradiation, again especially with 50 keV/μm carbon-ion beams.

For baseline correction, we used the normalized MN frequency to exclude the MN frequency in nonirradiated tumors. The normalized MN frequency was the MN frequency in the irradiated tumors minus that in the nonirradiated tumors. Dose-response curves of the normalized MN frequency for total and Q tumor cell populations as a function of radiation dose after γ-ray irradiation are shown in the left and right panels of Fig. 3, respectively. Overall, the normalized MN frequencies were significantly smaller in Q cells than in the total cells. In both total and Q cells, under RDR as well as HDR irradiation, the normalized MN frequencies increased in the following order: irradiation under totally hypoxic conditions < aerobic irradiation without drugs < irradiation after nicotinamide loading < irradiation after misonidazole loading. The normalized MN frequencies decreased with the decrease in dose rate under all conditions, especially irradiation after nicotinamide loading in the total cell population.

Dose-response curves of the normalized MN frequency for the total and Q tumor cells as a function of radiation dose after accelerated carbon-ion beam irradiation with an LET of 18 (Fig. 4) or 50 keV/μm (Fig. 5) are shown in the left and right panels, respectively. Overall, the normalized MN frequencies were significantly smaller in Q cells than total cells, but the differences in radiosensitivity between the total and Q cells were reduced compared with γ-ray irradiation, especially with 50 keV/μm carbon-ion beams. In both the total and Q cells, under RDR as well as HDR irradiation, the normalized MN frequencies increased in the same order as for γ-ray irradiation, but the degree of change was reduced, especially with 50 keV/μm carbon-ion beams. The decreases in the normalized MN frequency with the decrease in radiation dose rate were suppressed compared with γ-ray irradiation, again especially with 50 keV/μm carbon-ion beams.

To estimate the effect of aerobic irradiation compared with hypoxic irradiation in both the total and Q cells, the data for aerobic irradiation without any drug and irradiation under totally hypoxic conditions were used

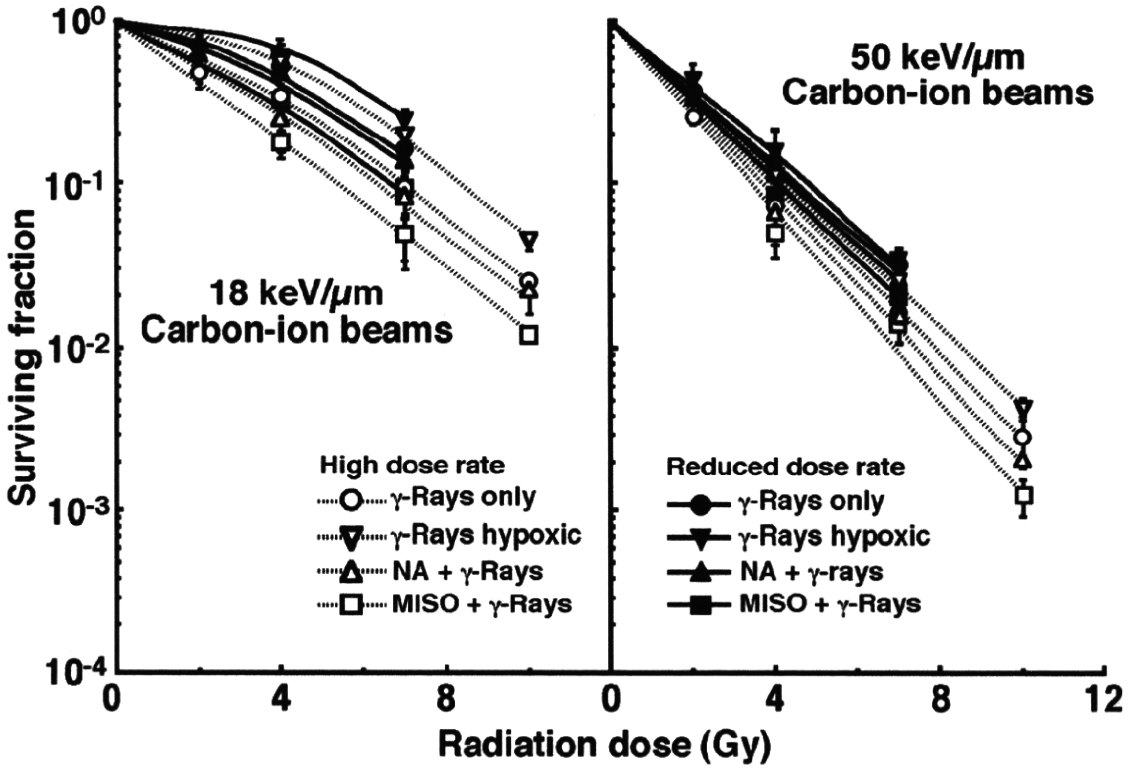

Fig. 2. Cell survival curves for the total tumor cell population as a function of the radiation dose after accelerated carbon-ion beam irradiation with linear energy transfers (LETs) of 18 and 50 keV/μm are shown in the *left* and *right panels*, respectively. Symbols are the same as defined in Fig. 1

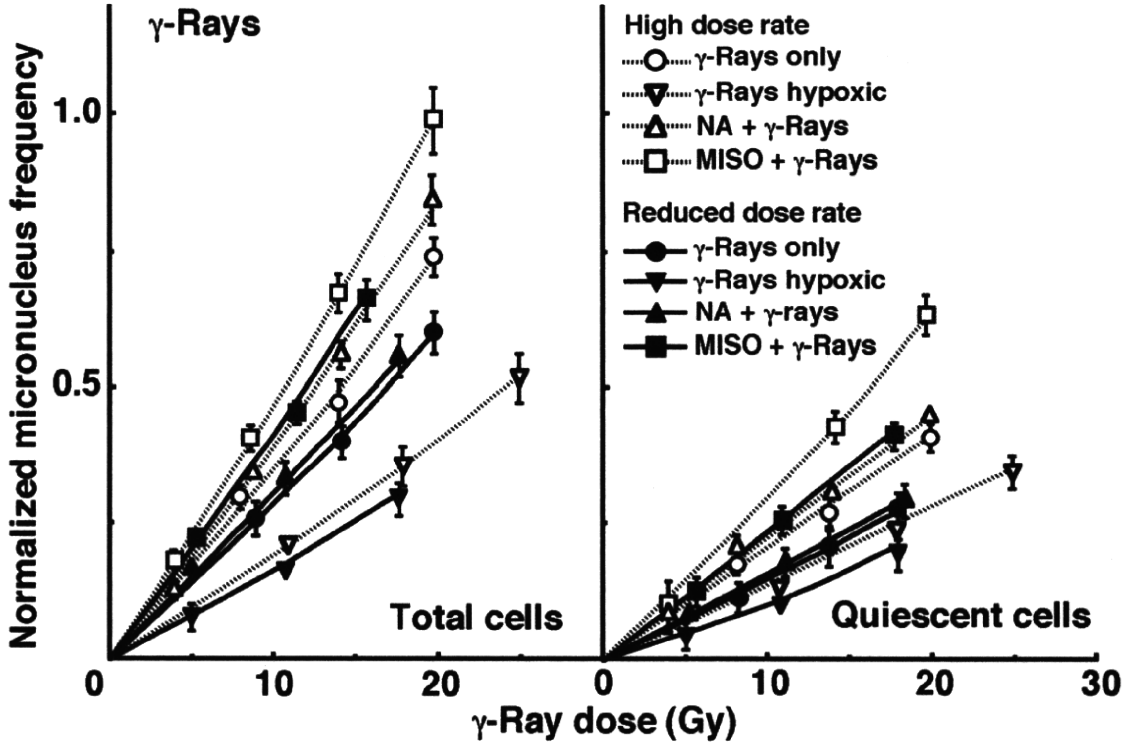

Fig. 3. Dose-response curves of the normalized micronucleus (MN) frequency for the total and quiescent tumor cell populations as a function of radiation dose after γ-ray irradiation are shown in the *left* and *right panels*, respectively. *Open* and *solid symbols* represent the normalized MN frequencies after high-dose-rate and reduced-dose-rate γ-ray irradiation, respectively. *Circles*, *reversed triangles*, *triangles*, and *squares* represent the normalized MN frequencies after aerobic irradiation without any drug, irradiation under totally hypoxic conditions, aerobic irradiation after nicotinamide (*NA*) loading, and aerobic irradiation after misonidazole (*MISO*) loading, respectively. *Bars* represent standard errors

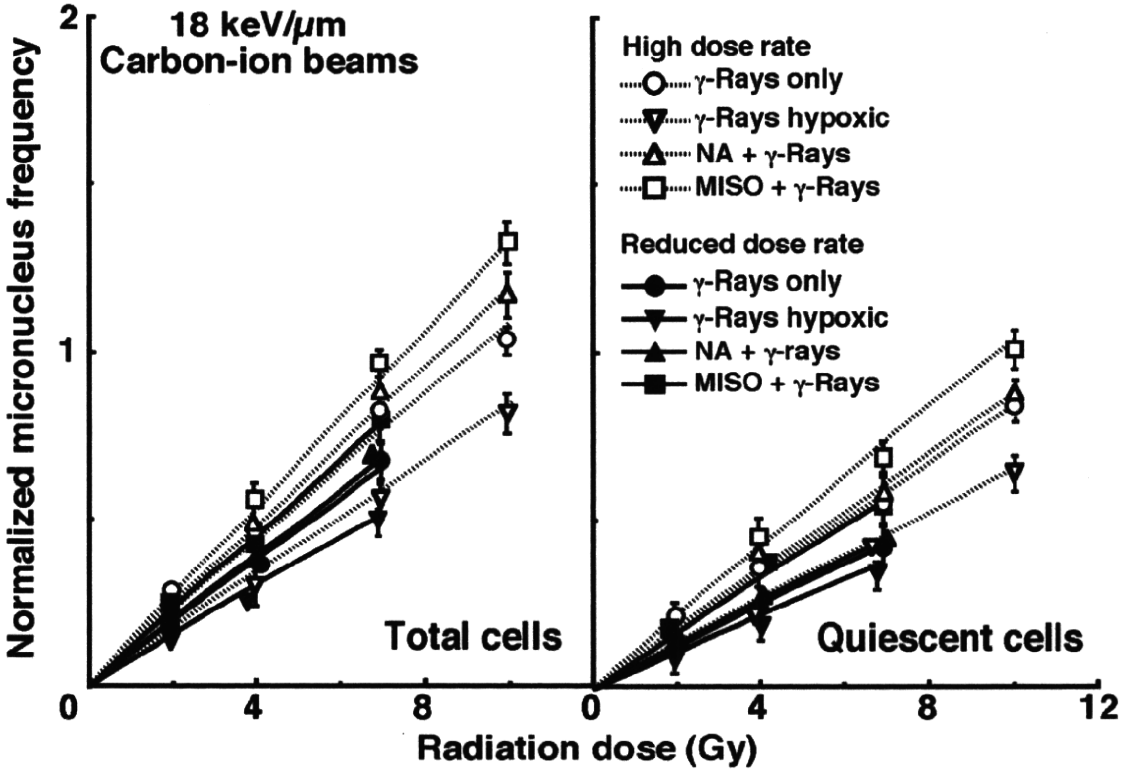

Fig. 4. Dose-response curves of the normalized MN frequency for the total and quiescent tumor cell populations as a function of radiation dose after accelerated carbon-ion beam irradiation with an LET of 18 keV/μm are shown in the *left* and *right panels*, respectively. *Open* and *solid symbols* represent the normalized MN frequencies after high-dose-rate and reduced-dose-rate accelerated carbon-ion beam irradiation, respectively. *Circles*, *reversed triangles*, *triangles*, and *squares* represent the normalized MN frequencies after aerobic irradiation without any drug, irradiation under totally hypoxic conditions, aerobic irradiation after nicotinamide (*NA*) loading, and aerobic irradiation after misonidazole (*MISO*) loading, respectively. *Bars* represent standard errors

Table 2. Irradiation under aerobic conditions compared with irradiation under hypoxic conditions[a]

Irradiation (γ-rays)	Carbon-ion beams (18 keV/μm)	Carbon-ion beams (50 keV/μm)
Surviving fraction = 0.3		
Total cells		
High dose: 2.1 (2.0–2.2)	1.4 (1.3–1.5)	1.15 (1.10–1.20)
Reduced dose: 1.8 (1.7–2.0)	1.25 (1.15–1.35)	1.10 (1.05–1.15)
Normalized micronucleus frequency = 0.2		
Total cells		
High dose: 1.9 (1.8–2.0)	1.35 (1.25–1.45)	1.2 (1.1–1.3)
Reduced dose: 1.7 (1.6–1.8)	1.25 (1.15–1.35)	1.15 (1.10–1.20)
Quiescent cells		
High dose: 1.5 (1.4–1.6)	1.25 (1.15–1.35)	1.15 (1.10–1.20)
Reduced dose: 1.3 (1.2–1.4)	1.10 (1.05–1.15)	1.05 (1.00–1.10)

Values in parentheses are 95% confidence limits, determined using standard errors. If the ranges of 95% confidence limits showed no overlap between any two values, the difference between the two values was considered significant ($P < 0.05$)

[a] The ratio of the dose of radiation necessary to obtain each endpoint under hypoxic conditions to that needed to obtain each endpoint under aerobic conditions

(Table 2). Following γ-ray irradiation, the values were significantly smaller for Q cells than for the total cells ($P < 0.05$), and in both the total and Q cells the values were significantly smaller for RDR than HDR irradiation ($P < 0.05$). In both populations, carbon-ion beams produced significantly smaller values than γ-rays ($P < 0.05$), and the values approached 1.0 as the LET values increased.

To assess the radio-enhancing effect of nicotinamide or misonidazole under aerobic conditions in both the

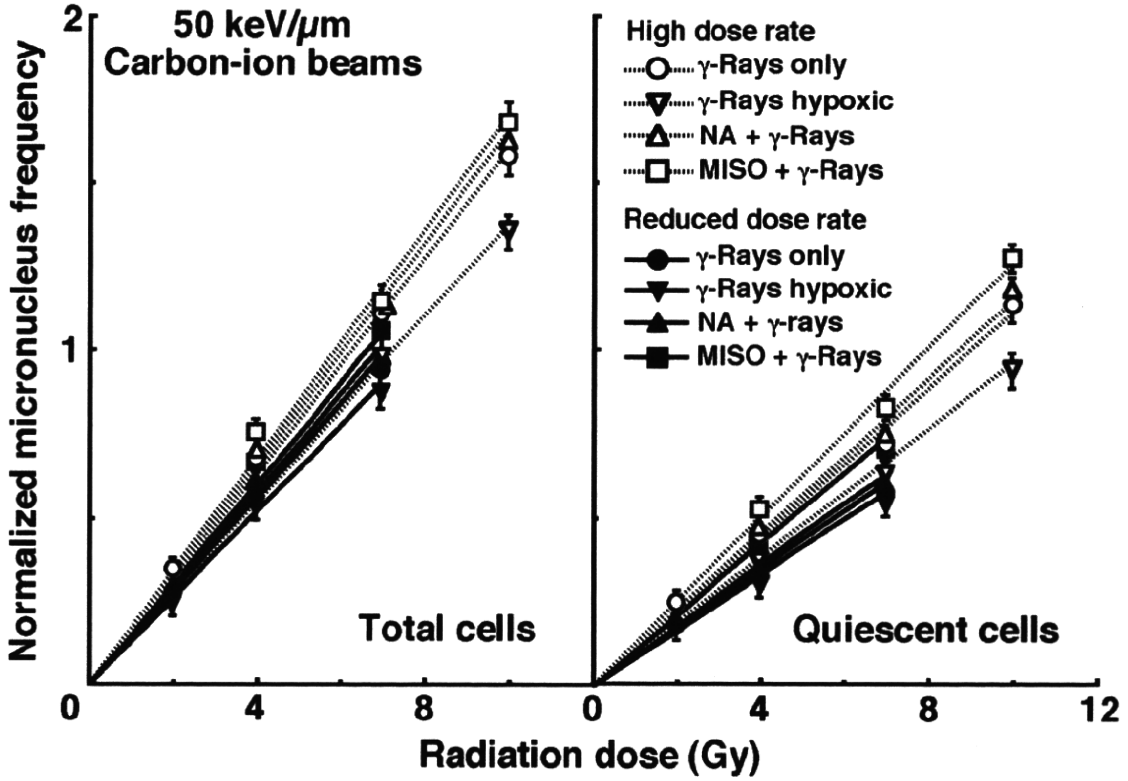

Fig. 5. Dose-response curves of the normalized MN frequency for the total and quiescent tumor cell populations as a function of radiation dose after accelerated carbon-ion beam irradiation with an LET of 50 keV/μm are shown in the *left* and *right panels*, respectively. Symbols are the same as defined in Fig. 4

total and Q cells compared with aerobic irradiation without any drug, the data for aerobic irradiation with and without drugs were used (Table 3). The enhancing effect of nicotinamide was more marked in the total cell population, especially with HDR γ-ray irradiation. The effect was little observed for RDR γ-ray irradiation and accelerated carbon-ion irradiation especially with a higher LET value. In contrast, the enhancing effect of misonidazole was more marked in the Q cells. The enhancing effect was also attenuated for accelerated carbon-ion irradiation, especially with a higher LET value.

To investigate the reduction in radiosensitivity caused by a decrease in the radiation dose rate, dose-modifying factors were calculated using the data for all irradiation conditions given in Figs. 1–5 (Table 4). On the whole, the reduction in radiosensitivity was more marked in Q cells than in the total cells, especially under γ-ray irradiation. In the total cells, the degree of the reduction of radiosensitivity was reduced in the following order: aerobic irradiation with nicotinamide > aerobic irradiation without any drug > aerobic irradiation with misonidazole > irradiation under totally hypoxic conditions. In Q cells, the degree of the reduction of radiosensitivity was reduced in the following order: aerobic irradiation with nicotinamide = aerobic irradiation without any drug > irradiation under totally hypoxic conditions > aerobic irradiation with misonidazole. This order of the reduction in radiosensitivity and the difference in the reduction in radiosensitivity between Q cells and the total cells became more indistinct with the use of accelerated carbon-ion beams, especially at a higher LET value, than with the use of γ-rays.

To examine the difference in radiosensitivity between the total and Q cells, dose-modifying factors—which allow us to compare the dose of radiation necessary to obtain a normalized MN frequency of 0.2 in Q cells with that in the total cells—were calculated using the data in Figs. 3–5 (Table 5). Overall, the difference in radiosensitivity was greater under RDR than HDR irradiation, especially with γ-rays. The difference in radiosensitivity increased in the following order: irradiation under totally hypoxic conditions < aerobic irradiation with misonidazole < aerobic irradiation without any drug ≤ aerobic irradiation with nicotinamide. This order of the increase in the difference in radiosensitivity and the difference itself in radiosensitivity became more indistinct with the use of accelerated carbon-ion beams, especially at a higher LET value, than with the use of γ-rays.

Table 3. Enhancement ratios[a] due to combination with nicotinamide or misonidazole

Parameter	High dose rate irradiation	Reduced dose rate irradiation
Surviving fraction = 0.3 (total cells)		
γ-Rays		
+ Nicotinamide	1.3 (1.2–1.4)[b]	1.05 (1.00–1.10)
+ Misonidazole	1.8 (1.6–2.0)	1.85 (1.70–2.00)
Carbon-ion beams (18 keV/μm)		
+ Nicotinamide	1.15 (1.10–1.20)	1.05 1.00–1.10)
+ Misonidazole	1.3 (1.2–1.4)	1.35 (1.30–1.40)
Carbon-ion beams (50 keV/μm)		
+ Nicotinamide	1.05 (1.00–1.10)	1.05 (1.00–1.10)
+ Misonidazole	1.10 (1.05–1.15)	1.15 (1.10–1.20)
Normalized micronucleus frequency = 0.2		
Total cells		
γ-Rays		
+ Nicotinamide	1.2 (1.1–1.3)	1.05 (1.00–1.10)
+ Misonidazole	1.3 (1.2–1.4)	1.35 (1.25–1.45)
Carbon-ion beams (18 keV/μm)		
+ Nicotinamide	1.15 (1.1–1.2)	1.05 (1.00–1.10)
+ Misonidazole	1.2 (1.1–1.3)	1.25 (1.15–1.35)
Carbon-ion beams (50 keV/μm)		
+ Nicotinamide	1.05 (1.00–1.10)	1.05 (1.00–1.10)
+ Misonidazole	1.05 (1.00–1.10)	1.05 (1.00–1.10)
Quiescent cells		
γ-Rays		
+ Nicotinamide	1.10 (1.05–1.15)	1.05 (1.00–1.10)
+ Misonidazole	1.45 (1.35–1.55)	1.5 (1.4–1.6)
Carbon-ion beams (18 keV/μm)		
+ Nicotinamide	1.05 (1.00–1.10)	1.00 (0.95–1.05)
+ Misonidazole	1.25 (1.15–1.35)	1.3 (1.2–1.4)
Carbon-ion beams (50 keV/μm)		
+ Nicotinamide	1.05 (1.00–1.10)	1.00 (0.95–1.05)
+ Misonidazole	1.10 (1.05–1.15)	1.10 (1.05–1.15)

Values in parentheses are 95% confidence limits, determined using standard errors. If the ranges of 95% confidence limits showed no overlap between any two values, the difference between the two values was considered significant ($P < 0.05$)

[a] The ratio of the dose of radiation necessary to obtain each end-point without the drug to that needed to obtain each end-point with the drug.

Table 4. Dose-modifying factors due to the reduction in radiosensitivity caused by a decrease in radiation dose rate[a]

γ-Rays	Carbon-ion beams (18 keV/μm)	Carbon-ion beams (50 keV/μm)
Surviving fraction = 0.3 (total cells)		
Radiation only: 1.3 (1.2–1.4)[b]	1.2 (1.1–1.3)	1.15 (1.10–1.20)
Totally hypoxic: 1.2 (1.1–1.3)	1.15 (1.05–1.25)	1.10 (1.05–1.15)
+ Nicotinamide: 1.55 (1.40–1.70)	1.35 (1.25–1.45)	1.20 (1.15–1.25)
+ Misonidazole: 1.25 (1.15–1.35)	1.2 (1.1–1.3)	1.15 (1.1–1.2)
Normalized micronucleus frequency = 0.2		
Total cells		
Radiation only: 1.25 (1.15–1.35)	1.2 (1.1–1.3)	1.10 (1.05–1.15)
Totally hypoxic: 1.15 (1.10–1.20)	1.10 (1.05–1.15)	1.05 (1.00–1.10)
+ Nicotinamide: 1.4 (1.25–1.55)	1.3 (1.2–1.4)	1.2 (1.1–1.3)
+ Misonidazole: 1.2 (1.1–1.3)	1.15 (1.05–1.25)	1.10 (1.05–1.15)
Quiescent cells		
Radiation only: 1.4 (1.3–1.5)	1.3 (1.2–1.4)	1.25 (1.15–1.35)
Totally hypoxic: 1.25 (1.15–1.35)	1.15 (1.10–1.20)	1.10 (1.05–1.15)
+ Nicotinamide: 1.4 (1.3–1.5)	1.3 (1.2–1.4)	1.25 (1.15–1.35)
+ Misonidazole: 1.15 (1.1–1.2)	1.10 (1.05–1.15)	1.10 (1.05–1.15)

Values in parentheses are 95% confidence limits, determined using standard errors. If the ranges of 95% confidence limits showed no overlap between any two values, the difference between the two values was considered significant ($P < 0.05$)

[a] The ratio of the dose of radiation necessary to obtain each end-point with reduced dose-rate irradiation to that needed to obtain each end-point with high dose-rate irradiation.

Table 5. Dose-modifying factors for quiescent cells relative to total tumor cells[a]

Normalized micronucleus frequency = 0.2 γ-rays	Carbon-ion beams (18 keV/μm)	Carbon-ion beams (50 keV/μm)
High dose rate irradiation		
Radiation only: 1.65 (1.5–1.8)	1.45 (1.35–1.55)	1.35 (1.25–1.45)
Totally hypoxic: 1.40 (1.15–1.55)	1.3 (1.2–1.4)	1.25 (1.15–1.35)
+ Nicotinamide: 1.75 (1.6–1.9)	1.5 (1.4–1.6)	1.4 (1.3–1.5)
+ Misonidazole: 1.50 (1.35–1.65)	1.35 (1.25–1.45)	1.3 (1.2–1.4)
Reduced dose rate irradiation		
Radiation only: 1.85 (1.70–2.00)	1.6 (1.5–1.7)	1.5 (1.4–1.6)
Totally hypoxic: 1.45 (1.35–1.55)	1.35 (1.25–1.45)	1.3 (1.2–1.4)
+ Nicotinamide: 1.85 (1.70–2.00)	1.6 (1.5–1.7)	1.5 (1.4–1.7)
+ Misonidazole: 1.55 (1.45–1.65)	1.4 (1.3–1.5)	1.35 (1.25–1.45)

Values in parentheses are 95% confidence limits, determined using standard errors. If the ranges of 95% confidence limits showed no overlap between any two values, the difference between the two values was considered significant ($P < 0.05$)

[a] The ratio of the dose of radiation necessary to obtain each normalized micronucleus frequency in quiescent cell population to that needed to obtain each normalized micronucleus frequency in total tumor cell population

Discussion

Solid tumors, especially human tumors, are thought to contain a high proportion of Q cells.[6] The presence of Q cells is probably due, in part, to hypoxia and depletion of nutrients in the tumor core, another consequence of poor vascular supply.[6] This might promote the formation of micronuclei at 0 Gy in Q tumor cells (Table 1). Q cells were shown to have significantly less radiosensitivity than the total cells here (Figs. 3–5). This means that more Q cells survive radiation therapy than P cells. Thus, control of Q cells has a great impact on the outcome of radiation therapy. In both the total and Q cell populations, carbon ion irradiation was less dependent on oxygenation status with little recovery from radiation-induced DNA damage, leading to high RBE values compared with γ-ray irradiation.[11] In terms of the tumor cell-killing effect as a whole, including intratumor Q cell control, carbon-ion beam radiotherapy can be a promising treatment for refractory tumors.

The Q cell population had been shown to include a significantly larger hypoxic fraction than the total cell population,[12] resulting in a significantly smaller effect of carbon-ion beams under aerobic irradiation compared with hypoxic irradiation in Q cells (Table 2). As tumor radiosensitivity was significantly less dependent on intratumor oxygenation status and the irradiation dose rate effect when carbon-ion beams, especially with a higher LET value, were used, a much smaller effect of aerobic irradiation compared with hypoxic irradiation was observed here. This was partly because the frequency of closely spaced DNA lesions forming a cluster of DNA damage produced by high-LET carbon-ion irradiation is much less dependent on oxygenation status at the time of irradiation than that of DNA damage produced by low-LET γ-ray irradiation.[13]

Tumor hypoxia is a direct consequence of structural abnormalities of the microvasculature and functional abnormalities of the microcirculation in solid tumors and results from either limited oxygen diffusion (chronic hypoxia) or limited perfusion (acute hypoxia, transient hypoxia, or ischemic hypoxia). Large intercapillary distances resulting from rapid tumor cell proliferation lead to chronically hypoxic cells existing at the rim of the oxygen diffusion distance.[14] Factors such as vessel plugging by blood cells or circulating tumor cells, the collapse of vessels in regions of high tumor interstitial pressure, and spontaneous vasomotor activity in normal tissue vessels incorporated into the tumor—which subsequently affects flow in downstream tumor microvessels—cause intermittent blood flow in tumors, which results in acute hypoxia.[15] Thus, acute hypoxic areas are distributed throughout the tumor depending on these causative factors and can occur sporadically in large areas of a solid tumor.

Nicotinamide, a vitamin B_3 analog, is known to prevent these transient fluctuations in tumor blood flow that lead to the development of acute hypoxia.[9] Misonidazole is a typical 2-nitro-imidazole hypoxic cell sensitizer that is thought to function as an oxygen-mimicking agent in intratumor hypoxic areas under irradiation.[10] In SCC VII tumors, it has been shown that the hypoxic fraction of the total cell population is predominantly made up of acute hypoxic areas and that of the hypoxia-rich Q cell population is mainly made up of chronic hypoxic areas.[12] Therefore, under HDR γ-ray irradiation, the enhancement ratio of nicotinamide was higher in the total cells than in Q cells, and that of misonidazole was higher in the Q cells (Table 3). When carbon-ion beams, especially with a higher LET value, were employed, these differences in the enhancement ratio were reduced because radiosensitivity was much less

dependent on intratumor oxygenation status.[11] However, under RDR γ-ray irradiation, acute hypoxic areas appear and disappear throughout a solid tumor during long periods of irradiation.[15] As a result, RDR irradiation even without nicotinamide could make it possible to irradiate all acute hypoxic areas under oxic conditions, leading to no radio-enhancing effect of nicotinamide. The radio-enhancing effect of misonidazole, which depends on the size of the hypoxic fraction in solid tumors, however, still could be observed under RDR as well as HDR irradiation.

Enhancement of the irradiation dose rate effect on the normalized frequency of micronuclei by γ-ray irradiation in the presence of nicotinamide compared with γ-ray irradiation alone was observed in the acute hypoxia-rich total cells rather than the chronic hypoxia-rich Q cells (Table 4). Suppression of the dose rate effect by inducing total hypoxia during irradiation was slightly more clearly observed in normoxia-rich total cells than hypoxia-rich Q cells. Some recent in vitro studies found that hypoxia-induced translational repression can explain the decreased homologous recombination (HR) repair of radiation-induced DNA double-stranded breaks (dsbs),[16] a more important mechanism for the repair of dsbs in late-S and G_2 growth phases, and that HR plays a greater role in determining hypoxic radiosensitivity than normoxic radiosensitivity.[17] Thus, the use of nicotinamide or tumor clamping to induce total hypoxia influenced repair more in the total cells including late-S and G_2 phase cells than in Q cells. In contrast, the repression of the dose rate effect by the hypoxic cell radiosensitizer misonidazole was slightly more clearly observed in the hypoxia-rich Q cells than in normoxia-rich total cells. It had already been shown that the loading of misonidazole after low-LET HDR irradiation to solid tumors inhibited the recovery from radiation-induced PLD in vivo, especially in Q cells.[18] This study showed that misonidazole combined with low-LET RDR irradiation could suppress the dose rate effect, especially in Q cells. According to the previous finding that the recovery from PLD and the decrease in radiosensitivity through a reduction in the irradiation dose rate under low-LET irradiation are mainly due to non-homologous end-joining (NHEJ) repair, which is the predominant DNA dsbs repair process for cells in G_0, G_1, or early-S phase,[19] misonidazole itself or protein adducts of reductively-activated misonidazole in hypoxic areas in irradiated tumors may inhibit NHEJ more efficiently than HR.[10] Again, when carbon-ion beams, especially with a higher LET value, were employed, the effects of combined treatment on the irradiation dose rate effect became indistinct because radiosensitivity was much less dependent on intratumor oxygenation status and the irradiation dose rate.[11]

Overall, the difference in radiosensitivity between the total and Q cells was increased by reducing the dose rate, especially for γ-ray irradiation, because of the greater reduction in radiosensitivity caused by a decrease in the dose rate in Q cells than in the total cells[9] (Table 5). Nicotinamide enhanced the radiosensitivity of the total cells, leading to widening of the difference in radiosensitivity between the total and Q cell populations compared with aerobic HDR γ-ray irradiation without any drug. However, for RDR γ-ray irradiation, the effect of nicotinamide disappeared owing to the characteristics of acute hypoxia in solid tumors, resulting in no change in the difference in radiosensitivity between the total and Q cells compared with γ-ray irradiation alone. Meanwhile, under totally hypoxic conditions, the difference in radiosensitivity was smaller than for aerobic γ-ray irradiation because of the radioresistance induced by total hypoxia in both the total and Q cell populations in sold tumors. Misonidazole enhanced the radiosensitivity of the hypoxia-rich Q cells much more than that of the total cells under both HDR and RDR γ-ray irradiation, leading to a decrease in the difference in radiosensitivity between the two cells compared with aerobic γ-ray irradiation alone. When carbon-ion beams, especially with a higher LET value, were employed, the effects of combined treatment on the difference in radiosensitivity between the total and Q cells became indistinct because tumor radiosensitivity was much less dependent on intratumor oxygenation status and the irradiation dose rate.[11] Anyway, at least in this study, it was elucidated that manipulating hypoxia during RDR irradiation, especially with γ-rays, influences tumor radiosensitivity as well as HDR irradiation in both total and Q cell populations. In radiotherapy, the irradiation dose rate also should be taken into account when intratumor hypoxia is manipulated.

Acknowledgments. This study was supported in part by a Grant-in-aid for Scientific Research (C) (20591493) from the Japan Society for the Promotion of Science.

References

1. Ahmed RS, Kim RY, Duan J, Meleth S, De Los Santos JF, Fiveash JB. IMRT dose escalation for positive para-aortic lymph nodes in patients with locally advanced cervical cancer while reducing dose to bone marrow and other organs at risk. Int J Radiat Oncol Biol Phys 2005;60:505–12.
2. Wulf J, Haedinger U, Oppitz U, Thiele W, Mueller G, Flentje M. Stereotactic radiotherapy for primary lung cancer and pulmonary metastases: a noninvasive treatment approach in medically inoperable patients. Int J Radiat Oncol Biol Phys 2004;60:186–96.
3. Hall EL, Giaccia AJ. Repair of radiation damage and the dose-rate effect. In: Hall EJ, Giaccia AJ, editors. Radiobiol-

ogy for the radiologist, 6th edn. Philadelphia: Lippincott Williams & Wilkins; 2006. p. 60–84.
4. Hall EL, Giaccia AJ. Linear energy transfer and relative biological effectiveness. In: Hall EJ, Giaccia AJ, editors. Radiobiology for the radiologist, 6th edn. Philadelphia: Lippincott Williams & Wilkins; 2006. p. 106–16.
5. Hall EL, Giaccia AJ. Oxygen effect and reoxygenation. In: Hall EJ, Giaccia AJ, editors. Radiobiology for the radiologist, 6th edn. Philadelphia: Lippincott Williams & Wilkins; 2006. p. 85–105.
6. Vaupel P. Tumor microenvironmental physiology and its implications for radiation oncology. Semin Radiat Oncol 2004;14:197–275.
7. Masunaga S, Ono K. Significance of the response of quiescent cell populations within solid tumors in cancer therapy. J Radiat Res 2002;43:11–25.
8. Torikoshi M, Minohara S, Kanematsu N, Komori M, Kanazawa M, Noda K, et al. Irradiation system for HIMAC. J Radiat Res 2007;48(suppl):A15–25.
9. Chaplin DJ, Horsman MR, Trotter MJ. Effect of nicotinamide on the microregional heterogeneity of oxygen delivery within a murine tumor. J Natl Cancer Inst 1990;82:672–6.
10. Wardman P. Chemical radiosensitizers for use in radiotherapy. Clin Oncol 2007;19:397–417.
11. Masunaga S, Ando K, Uzawa A, Hirayama R, Furusawa Y, Sakurai Y, et al. Radiobiologic significance of the response of intratumor quiescent cells in vivo to accelerated carbon ion beams compared with γ-rays and reactor neutron beams. Int J Radiat Oncol Biol Phys 2008;70:221–8.
12. Masunaga S, Ono K, Suzuki M, Nishimura Y, Hiraoka M, Kinashi Y, et al. Alteration of the hypoxic fraction of quiescent cell populations by hyperthermia at mild temperatures. Int J Hyperthermia 1997;13:401–11.
13. Hada M, Georgakilas AG. Formation of clustered DNA damage after high-LET irradiation: a review. J Radiat Res 2008;49:203–10.
14. Thomlinson RH, Gray LH. The histological structure of some human lung cancers and the possible implications for radiotherapy. Br J Cancer 1955;9:539–49.
15. Brown JM. Evidence of acutely hypoxic cells in mouse tumours and a possible mechanism of reoxygenation. Br J Radiol 1979;52:650–6.
16. Chan N, Koritzinsky M, Zhao H, Bindra R, Glazer PM, Powell S, et al. Chronic hypoxia decreases synthesis of homologous recombination proteins to offset chemoresistance and radioresistance. Cancer Res 2008;68:605–14.
17. Sprong D, Janssen HL, Vens C, Begg AC. Resistance of hypoxic cells to ionizing radiation is influenced by homologous recombination status. Int J Radiat Oncol Biol Phys 2006;64:562–72.
18. Masunaga S, Ono K, Abe M. Potentially lethal damage repair by quiescent cells in murine solid tumors. Int J Radiat Oncol Biol Phys 1992;22:973–8.
19. Masunaga S, Nagata K, Suzuki M, Kashino G, Kinashi Y, Ono K. Inhibition of repair from radiation-induced damage by mild temperature hyperthermia, referring to the effect on quiescent cell populations. Radiat Med 2007;25:417–25.

RADIATION RESEARCH 174, 459–466 (2010)
0033-7587/10 $15.00

DOI: 10.1667/RR2167.1

Evaluation of the Radiosensitivity of the Oxygenated Tumor Cell Fractions in Quiescent Cell Populations within Solid Tumors

Shin-ichiro Masunaga,[a,1] Hideko Nagasawa,[d] Yong Liu,[a] Yoshinori Sakurai,[b] Hiroki Tanaka,[b] Genro Kashino,[a] Minoru Suzuki,[a] Yuko Kinashi[c] and Koji Ono[a]

[a] *Particle Radiation Oncology Research Center,* [b] *Radiation Medical Physics and* [c] *Radiation Safety and Control, Research Reactor Institute, Kyoto University, 2-1010 Asashiro-nishi, Kumatori-cho, Sennan-gun, Osaka 590-0494, Japan; and* [d] *Laboratory of Pharmaceutical Chemistry, Gifu Pharmaceutical University, 1-25-4, Daigaku-nishi, Gifu 501-1196, Japan*

Masunaga, S., Nagasawa, H., Liu, Y., Sakurai, Y., Tanaka, H., Kashino, G., Suzuki, M., Kinashi, Y. and Ono, K. Evaluation of the Radiosensitivity of the Oxygenated Tumor Cell Fractions in Quiescent Cell Populations within Solid Tumors. *Radiat. Res.* 174, 459–466 (2010).

Labeling of all proliferating cells in C57BL/6J mice bearing EL4 tumors was achieved by continuous administration of 5-bromo-2′-deoxyuridine (BrdU). Tumors were irradiated with γ rays at a high dose rate or a reduced dose rate at 1 h after the administration of pimonidazole. Assessment of the responses of quiescent and total (= proliferating + quiescent) cell populations were based on the frequencies of micronucleation and apoptosis using immunofluorescence staining for BrdU. The response of the pimonidazole-unlabeled tumor cell fractions was assessed by means of apoptosis frequency using immunofluorescence staining for pimonidazole. The total cell fraction that was not labeled with pimonidazole showed significantly enhanced radiosensitivity. However, a significantly greater decrease in radiosensitivity, evaluated using a delayed assay or a decrease in radiation dose rate, was observed in the quiescent cell compared with the total cell population. Overall, the quiescent cell population showed significantly greater radioresistance and capacity to recover from radiation-induced damage than the total tumor cell population. Thus we believe that the subfraction of the quiescent tumor cell population that was not labeled with pimonidazole and that was probably oxygenated is a critical target in the control of solid tumors. © 2010 by Radiation Research Society

INTRODUCTION

Human solid tumors are thought to contain moderately large fractions of quiescent tumor cells, which are not involved in the cell cycle and have stopped dividing but which are as viable as established experimental animal tumor lines that are employed in oncology studies (*1*). The presence of quiescent cells is probably due at least in part to hypoxia and the depletion of nutrition as a consequence of poor vascular supply (*1*). As a result, with the exception of nonviable quiescent cells at the very edge of the necrotic rim where there is diffusion-limited hypoxia, quiescent cells are viable and clonogenic but have ceased dividing.

Using our method for selectively detecting the response of quiescent cells in solid tumors to treatment that damages DNA, the quiescent cell population in solid tumors has been shown to exhibit more resistance to conventional radio- and chemotherapy. The quiescent cell population has also been demonstrated to have more capacity to recover from radiation- and chemotherapy-induced damage and to have a significantly larger hypoxic fraction, especially a fraction that is chronically hypoxic, irrespective of the p53 status of tumor cells (*2*). However, the quiescent cell population in solid tumors has never been shown to be fully hypoxic (*2*). The sizes of the hypoxic fractions of the quiescent cell populations in SCC VII squamous cell carcinomas and EL4 leukemia cell tumors implanted in the hind legs of C3H/He and C57BL/6J mice and with a diameter of 1 cm were 55.1 ± 6.2% (mean ± SD) and 42.5 ± 5.4%, respectively (*3*). Thus the size of the hypoxic fraction in a quiescent cell population was significantly less than 100%. This finding indicated that the quiescent cell population undoubtedly includes oxygenated tumor cells.

A few years ago, the universal detection of hypoxic cells in both tissues and cell cultures became possible using pimonidazole, a substituted 2-nitroimidazole, and a mouse IgG1 monoclonal antibody (MAb1) to stable covalent adducts formed through reductive activation of pimonidazole in hypoxic cells (*1, 4*). In the present study, we endeavored to selectively examine the response of the pimonidazole-unlabeled and probably oxygenated fraction of the quiescent cell population. To achieve this we combined our method for selectively detecting the response of quiescent cells in solid tumors with a method for detecting cell and tissue hypoxia using pimonidazole and MAb1 to pimonidazole.

[1] Address for correspondence to: Particle Radiation Oncology Research Center, Research Reactor Institute, Kyoto University, 2-1010 Asashiro-nishi, Kumatori-cho, Sennan-gun, Osaka 590-0494, Japan; e-mail: smasuna@rri.kyoto-u.ac.jp.

Intensity-modulated radiotherapy and stereotactic irradiation have become common as modalities for the treatment of malignancies. Both approaches generally use multiple arc or fixed-portal radiation beams, and exposure to the radiation beams is intermittent. These techniques often require precise positioning of patients and exposure times of 30 min or longer in a single treatment session (*5, 6*). Prolongation of the irradiation time may induce adverse effects and raises major concerns related to the dose-rate effect. Thus there is a need to clarify the effect of a reduction in dose rate on the radiosensitivity of tumors *in vivo*. In the present study, the radiosensitivity of the pimonidazole-unlabeled fraction of the quiescent cell population after ^{60}Co γ irradiation at both a high dose rate and a reduced dose rate was determined. This represents the first attempt to evaluate the response of oxygenated fractions of quiescent tumor cells *in vivo*.

MATERIALS AND METHODS

Mice and Tumors

EL4 lymphoma (Cell Resource Center for the Biomedical Research Institute of Development, Aging and Cancer, Tohoku University) derived from C57BL/6J mice was maintained *in vitro* in RPMI 1640 medium supplemented with 12.5% fetal bovine serum. The p53 of the EL4 tumor cells was wild-type (*7*). Cells were collected from exponentially growing cultures, and approximately 1.0×10^5 tumor cells were inoculated subcutaneously into the left hind legs of 9-week-old syngeneic female C57BL/6J mice (Japan Animal Co., Ltd., Osaka, Japan). Fourteen days after inoculation the tumor had reached approximately 1 cm in diameter. The body weight of the tumor-bearing mice was 22.1 ± 2.3 g. Mice were handled according to the Recommendations for Handling of Laboratory Animals for Biomedical Research compiled by the Committee on Safety Handling Regulations for Laboratory Animal Experiments.

Labeling with 5-Bromo-2'-deoxyuridine (BrdU)

Nine days after tumor inoculation, mini-osmotic pumps (Durect Corporation, Cupertino, CA) containing BrdU dissolved in physiological saline (250 mg/ml) were implanted subcutaneously to enable the labeling of all proliferating cells over a 5-day period. The percentage of labeled cells after continuous labeling with BrdU was 66.1 ± 3.8% and had reached a plateau at this time. Therefore, tumor cells not incorporating BrdU after continuous labeling were regarded as quiescent cells.

Treatment

After labeling with BrdU, tumor-bearing mice received an intraperitoneal injection of pimonidazole hydrochloride (Hypoxyprobe Inc., Burlington, MA) dissolved in physiological saline at a dose of 60 mg/kg. Ninety minutes later mice were irradiated with γ rays without anesthesia. Individual animals were secured in a specially designed device made of acrylic resin with the tail firmly fixed with adhesive tape. Gamma rays were delivered using a ^{60}Co γ irradiator at dose rates of 2.5 and 0.039 Gy/min, representing a high dose rate and a reduced dose rate, respectively.

Each treatment group also included mice that had not been pretreated with BrdU.

Immunofluorescence Staining of BrdU-Labeled and/or Pimonidazole-Labeled Cells and the Observation of Apoptosis and Micronucleation

Based on our previous report related to the determination of the timing of apoptosis (*3*), an apoptosis assay undertaken at 6 h after irradiation and a micronucleus assay carried out immediately after irradiation were used as immediate assays. Tumors were excised from mice given BrdU, weighed, minced and trypsinized [0.05% trypsin and 0.02% ethylenediamine-tetraacetic acid (EDTA) in phosphate-buffered saline (PBS) at 37°C for 20 min]. As a delayed assay, tumors were also excised from mice given BrdU, weighed, minced and trypsinized at 30 h after irradiation for the apoptosis assay and at 24 h after irradiation for the micronucleus assay. For the apoptosis assay, single cell suspensions were fixed without further treatment. For the micronucleus assay, tumor cell suspensions were incubated for 72 h in tissue culture dishes containing complete culture medium and 1.0 μg/ml of cytochalasin B to inhibit cytokinesis while allowing nuclear division. The cultures were then trypsinized and cell suspensions were fixed in 75% ethanol. For both assays, after the centrifugation of fixed cell suspensions, the cell pellet was resuspended with cold Carnoy's fixative (ethanol:acetic acid = 3:1 in volume). The suspension was placed on a glass microscope slide, and the sample was dried at room temperature. Slides were treated with 2 *M* hydrochloric acid for 60 min at room temperature to dissociate the histones and partially denature the DNA. They were then immersed in borax-borate buffer (pH 8.5) to neutralize the acid. BrdU-labeled tumor cells were detected using indirect immunofluorescence staining with a rat monoclonal anti-BrdU antibody (Abcam plc, Cambridge, UK) and a goat Alexa Fluor 488-conjugated anti-rat IgG antibody (Invitrogen Corp., Carlsbad, CA). Pimonidazole-labeled tumor cells were identified using indirect immunofluorescence staining with a mouse monoclonal anti-pimonidazole antibody (Hypoxyprobe Inc., Burlington, MA) and a rabbit Alexa Fluor 594-conjugated anti-mouse IgG antibody (Invitrogen). To enable the observation of the triple staining of tumor cells with green-emitting Alexa Fluor 488 and red-emitting Alexa Fluor 594, cells on the slides were treated with blue-emitting 4'6-diamidino-2-phenylindole (DAPI) (0.5 μg/ml in PBS) and monitored under a fluorescence microscope.

The frequency of apoptosis in BrdU-unlabeled cells (= quiescent cells at irradiation) and pimonidazole-unlabeled tumor cells was determined by counting apoptotic cells in tumor cells that did not show green fluorescence from Alexa Fluor 488 and red fluorescence from Alexa Fluor 594, respectively. The apoptosis frequency was defined as the ratio of the number of apoptotic cells to the total number of observed tumor cells (*3*). The micronucleus frequency in BrdU-unlabeled cells was determined by counting the micronuclei in the binuclear cells that did not show green fluorescence emitted by Alexa Fluor 488. The micronucleus frequency was defined as the ratio of the number of micronuclei in the binuclear cells to the total number of binuclear cells observed (*2*).

The ratios obtained in tumors not pretreated with BrdU indicated the apoptosis frequency and the micronucleus frequency in the total (proliferating + quiescent) tumor cell populations. More than 300 tumor cells and binuclear cells were counted to determine the apoptosis frequency and the micronucleus frequency, respectively.

Clonogenic Cell Survival Assay

The clonogenic cell survival assay was also performed in the mice that were given no BrdU or pimonidazole using an *in vivo-in vitro* assay method. Tumors were disaggregated by stirring for 20 min at 37°C in PBS containing 0.05% trypsin and 0.02% EDTA. The cell yield was $(1.1 \pm 0.3) \times 10^8$/g tumor weight. A colony formation assay using the *in vivo-in vitro* assay method was performed with the culture medium mixed with methylcellulose (15.0 g/liter) (Aldrich, Milwaukee, WI).

The apoptosis and micronucleus frequencies and surviving fractions for the total cell population were obtained from cells in tumors

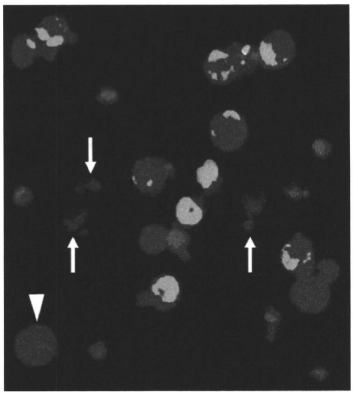

FIG. 1. Fluorescence photomicrograph showing triple-stained EL4 tumor cells with green fluorescence (FITC) indicating BrdU distribution, red fluorescence (Alexa 495) indicating pimonidazole distribution, and blue fluorescence (DAPI) indicating the background cell nucleus distribution. Arrows and arrowhead show apoptotic and non-apoptotic tumor cells without pimonidazole or BrdU.

that were not pretreated with BrdU or pimonidazole. The apoptosis and micronucleus frequencies for quiescent cells were obtained from unlabeled tumor cells after continuous BrdU labeling without pimonidazole loading. The apoptosis frequencies for the total tumor cell population that was not labeled with pimonidazole were obtained from tumor cells that were not labeled with pimonidazole after pimonidazole loading without BrdU pretreatment. The apoptosis frequencies for quiescent cells that were not labeled with pimonidazole were obtained from tumor cells that were not labeled with BrdU or pimonidazole after both continuous BrdU labeling and pimonidazole loading (Fig. 1). Thus there was no effect of the interaction between BrdU and radiation or between pimonidazole and radiation on apoptosis and micronucleus frequencies and the surviving fractions. Since the rate of pimonidazole-labeled tumor cells could change during culturing with cytochalasin B over 3 days, after the production of single tumor cell suspensions by excising and mincing the tumors from mice that underwent pimonidazole loading, the micronucleus frequency for the cell fraction that was not labeled with pimonidazole after pimonidazole loading was not determined. As a consequence, the radiosensitivity of the pimonidazole-unlabeled cell fractions was determined only in relation to apoptosis induction. This was the reason for using the EL4 leukemia cell line with its much greater capacity for the induction of apoptosis than cell lines that originated from solid tumors (*3*).

More than three tumor-bearing mice were used to assess each set of conditions, and each experiment was repeated at least twice. To examine the differences between pairs of values, Student's t test was used when variances of the two groups were assumed to be equal; otherwise the Welch t test was used.

RESULTS

The plating efficiency and the micronucleus and apoptosis frequencies in unirradiated cells are shown in Table 1. The micronucleus and apoptosis frequencies were significantly higher in the quiescent cell population than in the total cell population. In contrast, the apoptosis frequency was significantly lower in the cell fraction that was not labeled with pimonidazole than in the whole tumor cell fraction in both the quiescent and total tumor cell populations.

TABLE 1
Plating Efficiency and Micronucleus Frequency in Unirradiated Cells

	Total tumor cells	Quiescent cells
Plating efficiency (%)	25.5 ± 6.8[a]	—
Micronucleus frequency	0.053 ± 0.003	0.073 ± 0.006
Apoptosis frequency	0.040 ± 0.001	0.067 ± 0.004
In pimonidazole-unlabeled cell fraction	0.017 ± 0.001	0.028 ± 0.003

[a] Mean ± SD.

Cell survival curves for the total tumor cell population as a function of radiation dose are shown in Fig. 2. The surviving fractions (SFs) increased in the following order: immediately after high-dose-rate irradiation < 24 h after high-dose-rate irradiation < immediately after reduced-dose-rate irradiation.

For baseline correction we used the normalized micronucleus frequency to exclude the micronucleus frequency in nonirradiated tumors. The normalized micronucleus frequency was defined as the micronucleus frequency in the irradiated tumors minus the micronucleus frequency in the nonirradiated tumors. Dose–response curves for the normalized micronucleus frequency in the total and quiescent tumor cell populations as a function of radiation dose are shown in Fig. 3. Overall, the normalized micronucleus frequencies were significantly lower in the quiescent cell population than in the total cell population. In both the total and quiescent cell populations, the normalized micronucleus frequencies decreased in the following order: immediately after high-dose-rate irradiation > 24 h after high-dose-rate irradiation > immediately after reduced-dose-rate irradiation. The correlation between the normalized micronucleus frequency and the SF of the total tumor cell population under each set of irradiation conditions was examined. The regression line had a significant positive correlation ($P < 0.01$) (Fig. 4).

As another baseline correction we used the normalized apoptosis frequency to exclude the apoptosis frequency in nonirradiated tumors. The normalized apoptosis frequency was the apoptosis frequency in the irradiated tumors minus that in the nonirradiated tumors. Dose–response curves for the normalized apoptosis frequency in the total and quiescent tumor cell populations as a function of radiation dose are shown in Fig. 5. Overall, the normalized apoptosis frequencies were significantly lower in the quiescent cells than in the total cell population. In addition, the normalized apoptosis frequency was significantly higher for the cell fraction that was not labeled with

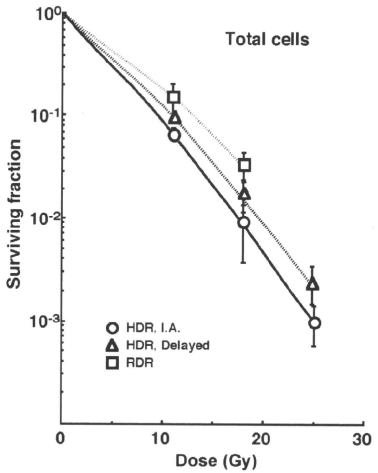

FIG. 2. Cell survival curves for the whole tumor cell fraction in the total tumor cell population as a function of radiation dose. Open and solid symbols represent the surviving fractions after high-dose-rate and reduced-dose-rate γ irradiation, respectively. Circles, triangles and squares represent the surviving fractions immediately after (I.A.) and at 24 h after (delayed) high-dose-rate (HDR) and reduced-dose-rate (RDR) γ irradiation, respectively. Bars represent standard errors.

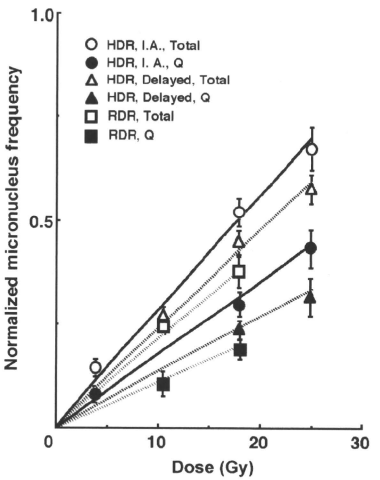

FIG. 3. Dose–response curves of the normalized micronucleus frequency for the whole tumor cell fraction in the total and quiescent tumor cell populations as a function of radiation dose. Open and solid symbols represent the normalized micronucleus frequencies for total and quiescent (Q) tumor cell populations, respectively. Circles, triangles and squares represent the normalized micronucleus frequency immediately after (I.A.) and at 24 h after (delayed) high-dose-rate (HDR) and reduced-dose-rate (RDR) γ irradiation, respectively. Bars represent standard errors.

pimonidazole than for the whole tumor cell fraction in both the quiescent and total tumor cell populations under each set of conditions. For both the pimonidazole-unlabeled and the whole cell fractions, in both the quiescent and total tumor cell populations, the normalized apoptosis frequencies decreased in the following order: immediately after high-dose-rate irradiation > 24 h after high-dose-rate irradiation > immediately after reduced-dose-rate irradiation. The correlation between the normalized apoptosis frequency and the SF of the total tumor cell population under each set of conditions was examined. The regression line had a significant positive correlation ($P < 0.015$) (Fig. 6).

To estimate of the radiosensitivity of the cell fraction that was not labeled with pimonidazole, compared with the whole cell fraction in both the total and quiescent cell populations, dose-modifying factors (DMFs) were calculated using the data obtained under all irradiation conditions (Fig. 5, Table 2). The DMFs were significantly higher than 1.0 under all conditions ($P < 0.05$). Overall, the DMFs were higher for the quiescent cells than for the total cell population, with the greatest difference immediately after high-dose-rate irradiation. In the total cell population, the DMFs were almost constant. However, for quiescent cells, the DMFs had a tendency to decrease in the following order: immediately after high-dose-rate irradiation > 24 h after high-dose-rate irradiation > immediately after reduced-dose-rate irradiation.

To investigate the reduction in radiosensitivity caused by a delayed assay or a decrease in the radiation dose rate, DMFs were calculated using the data for all irradiation conditions given in Figs. 2, 3 and 5 (Table 3). In the cell fraction unlabeled with pimonidazole or the whole cell fraction, the DMFs were higher after reduced-dose-rate irradiation than at 24 h after high-dose-rate irradiation in both the quiescent and total cell populations. The DMFs were significantly higher in the quiescent cells than the total cell population in both the pimonidazole-unlabeled and whole cell fractions. In both the quiescent and total cell populations, the values for pimonidazole-unlabeled cell fractions were higher than those for the whole cell fractions.

To examine the difference in radiosensitivity between the total and quiescent cell populations, DMFs, which allow us to compare the dose of radiation necessary to obtain each end point in the two cell populations, were calculated using the data in Figs. 3 and 5 (Table 4). All DMFs were significantly higher than 1.0 under each set of conditions (Table 4). The DMFs increased in the following order: immediately after high-dose-rate irradiation < 24 h after high-dose-rate irradiation <

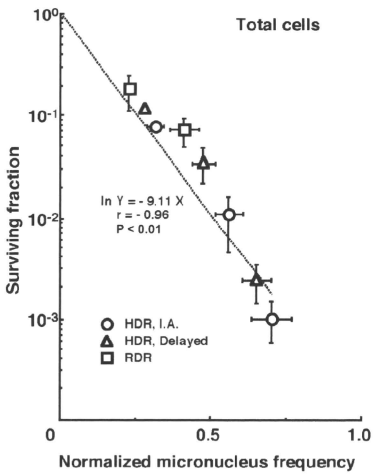

FIG. 4. Correlation between the normalized micronucleus frequency and the surviving fraction of the whole tumor cell fraction in the total tumor cell population for each tumor under each set of treatment conditions. The regression line had a significant positive correlation: ln $Y = -9.11X$ ($r = -0.96$, $P < 0.01$). Symbols are the same as in Fig. 3. Bars represent standard errors.

immediately after reduced-dose-rate irradiation. They were lower in the fraction of the cell population that was not labeled with pimonidazole in the quiescent cell population compared with the total cell fraction.

DISCUSSION

In recent years the concept of cancer stem cells, or tumor-initiating cells (tumor clonogens), has ignited a great deal of interest because of the potential clinical implications of these cells (*8*). In part, these cells are thought to exist in a pathophysiological microenvironment where hypoxia, low pH and nutrient deprivation occur. In addition, within the tumor microenvironment significant heterogeneity, both spatial and temporal, also occurs (*9*). These microenvironment conditions in the tumor can also cause dividing tumor cells to become quiescent (*1*). Furthermore, a subset of cancer stem cells or tumor clonogens is thought to consist of nondividing quiescent cells (*9*). Thus, in the present study, we attempted to clarify the radiobiological characteristics of this subpopulation of the quiescent cell population in the context of cancer stem cell or tumor clonogens.

As shown in Figs. 4 and 6, both the normalized micronucleus and apoptosis frequencies reflect radiosensitivity as precisely as the clonogenic survival curves for EL4 cells due to the fact that there is a statistically

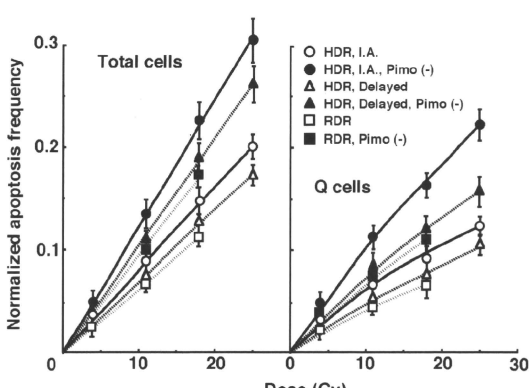

FIG. 5. Dose–response curves for the normalized apoptosis frequency of the total and quiescent (Q) tumor cell populations as a function of radiation dose are shown in the left and right panels, respectively. Open and solid symbols represent the normalized apoptosis frequencies for the whole tumor cell fraction and the cell fraction not labeled with pimonidazole (Pimo (-)) in both the total and quiescent tumor cell populations, respectively. Circles, triangles and squares represent the normalized apoptosis frequency immediately after (I.A.) and at 24 h after (delayed) high-dose-rate (HDR) and reduced-dose-rate (RDR) γ irradiation, respectively. Bars represent standard errors.

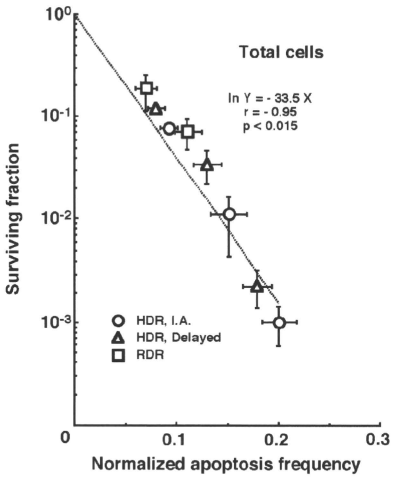

FIG. 6. Correlation between the normalized apoptosis frequency and the surviving fraction of the whole tumor cell fraction in the total tumor cell population for each tumor under each set of treatment conditions. The regression line had a significant positive correlation: $\ln Y = -33.5X$ ($r = -0.95$, $P < 0.015$). Symbols are the same as those detailed in Fig. 5. Bars represent standard errors.

significant positive correlation with the SF. The fraction of cells that were not labeled with pimonidazole showed significantly greater radiosensitivity than the whole cell fraction in both the quiescent and total cell populations,

TABLE 2
Dose-Modifying Factors for the Pimonidazole Unlabeled Cell Fraction Compared with the Whole Cell Fraction in the Total or Quiescent Cell Population[a]

	High dose rate		
	Immediately after	24 h after	Reduced dose rate
Normalized apoptosis frequency = 0.06			
Total cell population	1.5 (1.4–1.6)[b]	1.5 (1.4–1.6)	1.55 (1.45–1.65)
Quiescent cell population	1.7 (1.6–1.8)	1.65 (1.55–1.75)	1.6 (1.5–1.7)
Normalized apoptosis frequency = 0.1			
Total cell population	1.5 (1.4–1.6)	1.5 (1.4–1.6)	1.5 (1.4–1.6)
Quiescent cell population	1.75 (1.65–1.85)	1.65 (1.55–1.75)	——

[a] The ratio of the dose of radiation necessary to obtain each end point in a whole cell fraction to that needed to obtain each end point in the pimonidazole-unlabeled cell fraction.

[b] Values in parentheses are 95% confidence limits, determined using standard errors. When the ranges of 95% confidence limits showed no overlap between two values, the difference between the two values was significant ($P < 0.05$) based on a χ^2 test.

TABLE 3
Dose-Modifying Factors Obtained Using a Delayed Assay or a Reduced Radiation Dose Rate[a]

	High dose rate 24 h after	Reduced dose rate
Surviving fraction = 0.05		
Total cells	1.15 (1.1–1.2)[b]	1.35 (1.25–1.45)
Normalized micronucleus frequency = 0.2		
Total cells	1.2 (1.1–1.3)	1.35 (1.25–1.45)
Quiescent cells	1.4 (1.3–1.5)	1.6 (1.45–1.75)
Normalized apoptosis frequency = 0.06		
Total cells	1.15 (1.1–1.2)	1.3 (1.2–1.4)
In pimonidazole-unlabeled cell fraction	1.2 (1.1–1.3)	1.3 (1.2–1.4)
Quiescent cells	1.35 (1.25–1.45)	1.55 (1.45–1.65)
In pimonidazole-unlabeled cell fraction	1.45 (1.35–1.55)	1.65 (1.5–1.8)

[a] The ratio of the dose of radiation necessary to obtain each end point with a delayed assay or reduced dose-rate irradiation to that needed to obtain each end point with an assay immediately after high dose-rate irradiation.

[b] Values in parentheses are 95% confidence limits, determined using standard errors. When the ranges of 95% confidence limits showed no overlap between two values, the difference between the two values was significant ($P < 0.05$) based on a χ^2 test.

and for the quiescent cells in particular (Table 2). This was probably because pimonidazole-unlabeled cells were more oxygenated than the whole cell fraction, which includes both oxygenated and hypoxic tumor cells, in both the quiescent and total tumor cell populations (*4*). Additionally the quiescent cell population included a much larger hypoxic fraction than the total tumor cell population (*3*). As shown in Table 3, the pimonidazole-

TABLE 4
Dose-Modifying Factors for Quiescent Cells Relative to Total Tumor Cells[a]

	High dose rate		
	Immediately after	24 h after	Reduced dose rate
Normalized micronucleus frequency = 0.2	1.65 (1.5–1.8)[b]	1.8 (1.65–1.95)	1.9 (1.75–2.05)
Normalized apoptosis frequency = 0.06	1.3 (1.2–1.4)	1.45 (1.35–1.55)	1.55 (1.4–1.7)
In pimonidazole-unlabeled cell fraction	1.2 (1.1–1.3)	1.4 (1.3–1.5)	1.55 (1.4–1.7)

[a] The ratio of the dose of radiation necessary to obtain each end point in the quiescent cell population to that needed to obtain each end point in the total tumor cell population.

[b] Values in parentheses are 95% confidence limits, determined using standard errors. When the ranges of 95% confidence limits showed no overlap between two values, the difference between the two values was significant ($P < 0.05$) based on a χ^2 test.

unlabeled cell fraction had a greater repair capacity than the whole cell fraction, especially in the case of the quiescent cells. As demonstrated in our previous study (*10*), radiosensitivity decreased in the following order: immediately after high-dose-rate irradiation, at 24 h after high-dose-rate irradiation and immediately after reduced-dose-rate irradiation, with greater changes in the quiescent cells (Table 3). As a consequence, in the case of the quiescent cells, the difference in radiosensitivity between the pimonidazole-unlabeled and whole cell fractions decreased in the same order. One mechanism of cancer stem cell or tumor clonogen resistance to cytotoxic treatment was reported to be related to an enhanced DNA repair capacity (*11*). Here the pimonidazole-unlabeled quiescent cell fraction showed a much greater repair capacity than the quiescent cell population considered as a whole, even though the repair capacity was significantly greater in the entire quiescent cell population than in the total tumor cell population as a whole. In other words, from the viewpoint of not only quiescent status but also enhanced DNA repair capacity, the characteristics of the pimonidazole-unlabeled cell fraction in the quiescent cell population were found to be similar to those of cancer stem cells or tumor clonogens.

The microenvironmental conditions under which dividing tumor cells become quiescent might promote the formation of micronuclei and apoptosis at 0 Gy in the whole quiescent tumor cell fractions, partly due to hypoxic stress (Table 1) (*1*). In the present study, the quiescent cells were shown to be significantly less radiosensitive and to have a greater repair capacity than the total cell population (Figs. 3 and 5, Tables 3 and 4). This finding indicated that more quiescent cells survive after radiation therapy than proliferating cells. In particular, in the cell fraction that was not labeled with pimonidazole, the difference in radiosensitivity between the quiescent and total cell populations was markedly increased when evaluated using the delayed assay or by employing a reduced radiation dose rate. This was due to the greater repair capacity of the unlabeled quiescent cell fraction compared with the unlabeled cell fraction in the total population (Table 4). Thus control of the quiescent cells could have a great impact on the outcome of radiation therapy and the quiescent cell population may be a critical target in the control of solid tumors.

Improving the oxygenation status in cultured tumor cells and solid tumors after irradiation has been shown to promote recovery from radiation-induced damage (*12–14*). In line with these findings, we found in the present study that the pimonidazole-unlabeled, and probably oxygenated, cell fraction showed a greater repair capacity than the quiescent cell population as a whole. However, although there were similarities between the pimonidazole-unlabeled quiescent cell fraction and cancer stem cells or tumor clonogens in terms of quiescent status and enhanced repair capacity, cancer stem cells or tumor clonogens are thought to exist under rather hypoxic conditions (*9*). As a consequence, in a future study that will include the use of human tumor cell lines, it will be necessary to further analyze the characteristics of the intratumor quiescent cell population in relation to those of cancer stem cells or tumor clonogens.

ACKNOWLEDGMENT

This study was supported in part by a Grant-in-aid for Scientific Research (C) (20591493) from the Japan Society for the Promotion of Science.

Received: February 8, 2010; accepted: June 7, 2010; published online: August 12, 2010

REFERENCES

1. P. Vaupel, Tumor microenvironmental physiology and its implications for radiation oncology. *Semin. Radiat. Oncol.* **206**, 198–206 (2004).
2. S. Masunaga and K. Ono, Significance of the response of quiescent cell populations within solid tumors in cancer therapy. *J. Radiat. Res.* **43**, 11–25 (2002).
3. S. Masunaga, K. Ono, M. Suzuki, Y. Kinashi and M. Takagaki, Radiobiologic significance of apoptosis and micronucleation in quiescent cells within solid tumors following γ-ray irradiation. *Int. J. Radiat. Oncol. Biol. Phys.* **49**, 1361–1368 (2001).
4. A. S. Ljungkvist, J. Bussink, P. F. Rijken, J. A. Raleigh, J. Denekamp and A. J. Van der Kogel, Changes in tumor hypoxia measured with a double hypoxic marker technique. *Int. J. Radiat. Oncol. Biol. Phys.* **48**, 1529–1538 (2000).
5. R. S. Ahmed, R. Y. Kim, J. Duan, S. Meleth, J. F. de los Santos and J. B. Fiveash, IMRT dose escalation for positive para-aortic lymph nodes in patients with locally advanced cervical cancer while reducing dose to bone marrow and other organs at risk. *Int. J. Radiat. Oncol. Biol. Phys.* **60**, 505–512 (2004).
6. J. Wulf, U. Haedinger, U. Oppitz, W. Thiele, G. Mueller and M. Flentje, Stereotactic radiotherapy for primary lung cancer and pulmonary metastases: a noninvasive treatment approach in medically inoperable patients. *Int. J. Radiat. Oncol. Biol. Phys.* **60**, 186–196 (2004).
7. S. Masunaga, K. Ono, M. Suzuki, Y. Nishimura, Y. Kinashi, M. Takagaki, H. Hori, H. Nagasawa, Y. Uto and C. Murayama, Radiosensitization effect by combination with paclitaxel *in vivo* including the effect on intratumor quiescent cells. *Int. J. Radiat. Oncol. Biol. Phys.* **50**, 1063–1072 (2001).
8. C. A. O'Brien, A. Kreso and J. E. Dick, Cancer stem cells in solid tumors: an overview. *Semin. Radiat. Oncol.* **19**, 71–76 (2009).
9. R. P. Hill, D. T. Marie-Egyptienne and D. W. Hedley, Cancer stem cells, hypoxia and metastasis. *Semin. Radiat. Oncol.* **19**, 106–111 (2009).
10. S. Masunaga, K. Ando, A. Uzawa, R. Hirayama, Y. Furusawa, Y. Sakurai, K. Nagata, M. Suzuki, G. Kashino and K. Ono, Radiobiological significance of the response of intratumor quiescent cells *in vivo* to accelerated carbon ion beams compared with gamma-rays and reactor neutron beams. *Int. J. Radiat. Oncol. Biol. Phys.* **70**, 221–228 (2008).
11. M. Diehn, R. W. Cho and M. F. Clarke, Therapeutic implications of the cancer stem cell hypothesis. *Semin. Radiat. Oncol.* **19**, 78–85 (2009).
12. D. Sprong, H. L. Janssen, C. Vens and A. C. Begg, Resistance of hypoxic cells to ionizing radiation is influenced by homologous recombination status. *Int. J. Radiat. Oncol. Biol. Phys.* **64**, 562–572 (2006).

13. N. Chan, M. Koritzinsky, H. Zhao, R. Bindra, P. M. Glazer, S. Powell, A. Belmaaza, B. Wouters and R. G. Bristow, Chronic hypoxia decreases synthesis of homologous recombination proteins to offset chemoresistance and radioresistance. *Cancer Res.* **68**, 605–614 (2008).

14. S. Masunaga, R. Hirayama, A. Uzawa, G. Kashino, M. Suzuki, Y. Kinashi, Y. Liu, S. Koike, K. Ando and K. Ono, The effect of postirradiation tumor oxygenation status on recovery from radiation-induced damage *in vivo*: with reference to that in quiescent cell populations. *J. Cancer Res. Clin. Oncol.* **135**, 1109–1116 (2009).